ACS Infectious Diseases

pubs.acs.org/journal/aidcbc

Article

Glycomic Analysis Reveals a Conserved Response to Bacterial Sepsis Induced by Different Bacterial Pathogens

Published as part of the ACS Infectious Diseases virtual special issue "Glycoscience in Infectious Diseases".

Daniel W. Heindel, Shuhui Chen, Peter V. Aziz, Jonathan Y. Chung, Jamey D. Marth, and Lara K. Mahal*

Cite This: *ACS Infect. Dis.* 2022, 8, 1075−1085

Read Online

ACCESS | Metrics & More | Article Recommendations | Supporting Information

ABSTRACT: Sepsis is an extreme inflammatory response to infection that occurs in the bloodstream and causes damage throughout the body. Glycosylation is known to play a role in immunity and inflammation, but the role of glycans in sepsis is not well-defined. Herein, we profiled the serum glycomes of experimental mouse sepsis models to identify changes induced by 4 different clinical bacterial pathogens (Gram-positive: *Streptococcus pneumoniae* and *Staphylococcus aureus*, Gram-negative: *Escherichia coli* and *Salmonella* Typhimurium) using our lectin microarray technology. We observed global shifts in the blood sera glycome that were conserved across all four species, regardless of whether they were Gram positive or negative. Bisecting GlcNAc was decreased upon sepsis and a strong increase in core 1/3 *O*-glycans was observed. Lectin blot analysis revealed a high molecular weight protein induced in sepsis by all four bacteria as the major cause of the core 1/3 *O*-glycan shift. Analysis of this band by mass spectrometry identified interalpha-trypsin inhibitor heavy chains (ITIHs) and fibronectin, both of which are associated with human sepsis. Shifts in the glycosylation of these proteins were observed. Overall, our work points toward a common mechanism for bacterially induced sepsis, marked by conserved changes in the glycome.

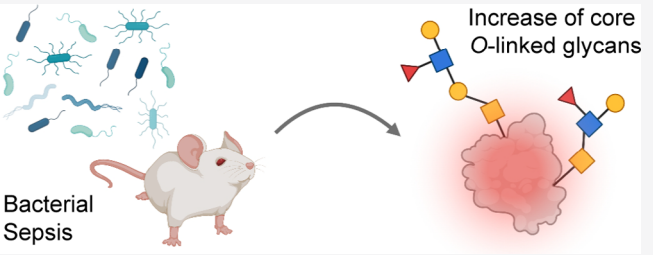

KEYWORDS: *serum glycomics, core 1/3 O-glycans, lectin microarray, sepsis, interalpha-trypsin inhibitor heavy chains (ITIHs), fibronectin*

Sepsis is classified as an infection of the bloodstream that is associated with pathological inflammation and organ system dysfunction.[1] Currently, few diagnostic biomarkers and effective targeted therapies exist.[1,2] A better understanding of the host-response and pathogenic mechanisms associated with disease onset and progression are required for developing more effective treatment strategies. Both Gram-positive and Gram-negative bacteria have been identified as common pathogens in septic patients. Incidence of sepsis driven by bacteria has increased in recent years, associated with the development of antibiotic resistance.[3,4] Bacteria initiate an innate immune response through host recognition of pathogen-associated molecular patterns (PAMPs). Examples of bacterial PAMPs include lipoteichoic acid (a component of the cell wall of Gram-positive bacteria) and lipopolysaccharide (expressed by Gram-negative bacteria) as well as constituents expressed by both Gram-positive and Gram-negative bacteria (peptidoglycan). These PAMPs initiate an inflammatory response through recognition by Toll-like receptors (TLRs). Uncontrolled stimulation of TLRs results in excessive inflammation associated with the septic phenotype.[5]

Glycosylation is known to play a role in immunity and inflammation.[6] Innate immune lectins can recognize glycan structures on the surface of bacteria and signal an immune response. Inflammatory cytokines can shift cell surface *N*-glycosylation of endothelial cells, contributing to inflammatory vascular diseases.[7,8] Recent work demonstrated that shifts in the glycan structure of a single glycoprotein in the context of discrete pathogens could help drive a septic state specific to Gram-positive bacteria in a TLR4-dependent manner.[9] However, whether such glycomic shifts are observable at the global level is unknown.

Herein, we examined the global glycosylation profile of blood sera in mouse models of experimental sepsis. Previous studies have indicated that mouse models closely mimic human responses in inflammatory diseases.[10] We focused our

Received: February 8, 2022
Published: April 29, 2022

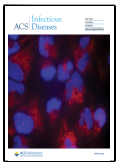

work on sepsis induced by four different clinical isolates of bacterial pathogens: Gram-positive *Streptococcus pneumoniae* (SPN), methicillin-resistant *Staphylococcus aureus* (MRSA), Gram negative *Escherichia coli* (EC), and *Salmonella enterica* Typhimurium (ST). Sera from control as well as early and late sepsis time points were analyzed using our dual-color lectin microarray technology.[11] This technology has been used to perform glycomics on a wide variety of samples including exosomes,[12,13] cervical lavage samples[14] and human tumor tissues.[15,16] Our glycomic analysis revealed two conserved changes occurring upon sepsis triggered by both Gram-positive and Gram-negative bacteria, a loss of bisecting GlcNAc and a dramatic increase in core 1/3 *O*-glycans. Lectin blot analysis confirmed our findings and showed induction of a single band at high molecular weight protein associated with the core 1/3 *O*-glycan signature. Glycoproteomic analysis of this band identified several glycoproteins including interalpha-trypsin inhibitor heavy chains (ITIHs) and fibronectin, both of which are associated with human sepsis. Shifts in the glycosylation of these proteins were observed with sepsis, suggesting an unexplored role for glycosylation in sepsis biology. Overall, our work identifies a common feature of bacterially induced sepsis, marked by conserved changes in the glycome.

RESULTS AND DISCUSSION

Description of Experimental Sepsis Models. Although glycosylation plays important roles in infection and host-response, there is little known about overall glycomic changes in sera in response to bacterial sepsis. Recent studies on the glycosylation of specific glycoproteins in mouse models found associations between glycosylation and different mechanisms of sepsis caused by Gram-positive and Gram-negative bacteria.[9,17,18] However, whether this translates into broader glycomic alterations in sera due to sepsis was not explored. To address this issue, we analyzed sera from a previously published experimental sepsis study.[9] In this study, mice were infected with clinical isolates of bacterial strains that commonly induce sepsis: *Methicillin-resistant Staphylococcus aureus* (MRSA), *Streptococcus pneumoniae* (SPN), Escherichia *coli* (EC), and *Salmonella enterica* Typhimurium (ST). For each pathogen early and late postinfection time points (early and late sepsis), corresponding to colony forming units (cfu) thresholds, were analyzed (Scheme 1). A total of 48 mice were studied per bacterial species, with equal numbers of female and male mice (n = 8 per sex per group: uninfected, preseptic, septic, n = 16 total for each condition).

Scheme 1. Murine Model of Sepsis[a]

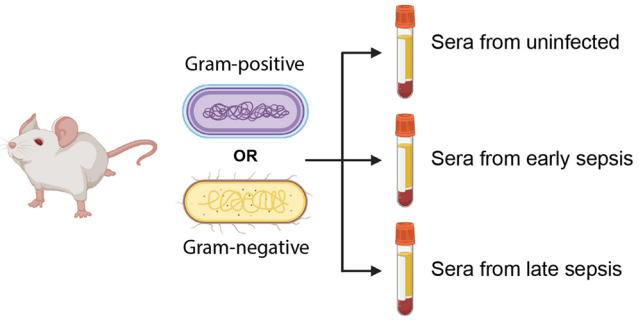

[a]Sera were collected from uninfected mice, and all comparisons were made to this group for each type of bacteria. Blood was collected at specified times postinfection to determine bacterial cfu for both early and late stages of sepsis as described.[9]

Lectin Microarray Analysis of Glycomic Response to Bacterial Sepsis from Gram-Positive Bacteria. The Gram-positive species *Streptococcus pneumoniae* (SPN) and Methicillin-resistant *Staphylococcus aureus* (MRSA) have both been named as priority pathogens by the World Health Organization because of their high burden of disease and antibiotic resistance.[19] Both of these clinical isolates are common causes of human sepsis. *Streptococcus pneumoniae* (SPN) commonly colonizes mucosal surfaces of the human upper respiratory tract, and is a major cause of community-acquired pneumonia.[20] Methicillin-resistant *Staphylococcus aureus* (MRSA) is an antibiotic resistant variant of a bacteria commonly found on the skin and in the upper respiratory tract. MRSA is a leading cause of bacterial infections in health-care and community settings. To look for glycomic signatures associated with bacterial sepsis caused by these organisms, we analyzed sera samples from our mouse models of experimental sepsis using our dual-color lectin microarray technology (Scheme 2).[11,21]

Lectin microarrays display immobilized carbohydrate binding proteins with known glycan specificities to detect glycomic variations between samples.[11,14,21,22] In brief, sera samples (sample) and a bacteria-specific pooled reference (reference) were labeled with orthogonal fluorescent dyes. Equal amounts of protein (7 μg each) of sample and reference were analyzed on the lectin microarray (>100 lectins, see Table S1 for printlist). Only lectins passing our quality control are shown. Heatmaps displaying the normalized data for Gram-positive bacterial species (SPN and MRSA) are shown in Figure 1 and Supplementary Figures S1 and S2.

Although SPN and MRSA have different colonization patterns and tropism, we observed a remarkably consistent glycomic response by the host to sepsis induced by both pathogens when compared to the corresponding uninfected controls (Figure 1, Supplementary Figures S3 and S4). The most striking change was a significant increase in core 1/3 *O*-Glycans (lectins: MPA, AIA, MNA-G, SPN: ∼2−3-fold increase, p = 0.0007, MRSA: ∼5-fold increase, $p = 2 \times 10^{-8}$, increase based on MPA). This observation is discussed in more detail below. We also observed a decrease in bisecting GlcNAc, which was more dramatic in the MRSA-infected animals (PHA-E, SPN: ∼1.5-fold decrease, p = 0.1, MRSA: ∼1.5-fold decrease, p = 0.0001). The reduction of bisecting GlcNAc was detected at both early and late sepsis time points, indicating that this change occurs early in progression of sepsis (Supplementary Figure S5). Although the meaning of this change is unclear, it is of note that bisecting GlcNAc has a known role in IgG biology and is found on ∼10% of all human IgG.[23,24] When on the Fc region of IgG, this glycan epitope increases affinity for the Fcγ3a receptor, leading to enhanced antibody dependent cellular cytotoxicity (ADCC). During sepsis, a loss of IgG correlates with an increase in mortality.[25] Whether the reduction of this glycan structure is due to altered IgG levels or other glycoproteins remains to be examined.

Lectin Microarray Analysis of Glycomic Response to Bacterial Sepsis from Gram-Negative Bacteria. The severity of inflammation in sepsis induced by Gram-negative bacteria has been shown to be higher than that of Gram-positive bacteria.[26] The gut pathogens *Salmonella enterica* Typhimurium (ST) and *Escherichia coli* (EC) used in our studies are clinical isolates and common causes of human sepsis.[27,28] To explore the glycomic response to Gram-negative

https://doi.org/10.1021/acsinfecdis.2c00082
ACS Infect. Dis. 2022, 8, 1075−1085

Scheme 2. Lectin Microarray Workflow[a]

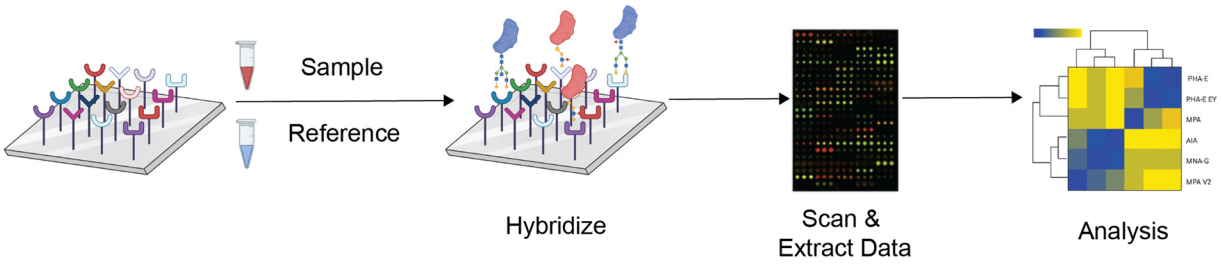

[a]Equal protein amounts (7 μg) for each sample and an orthogonally labeled mixed reference were combined and analyzed on the lectin microarray.

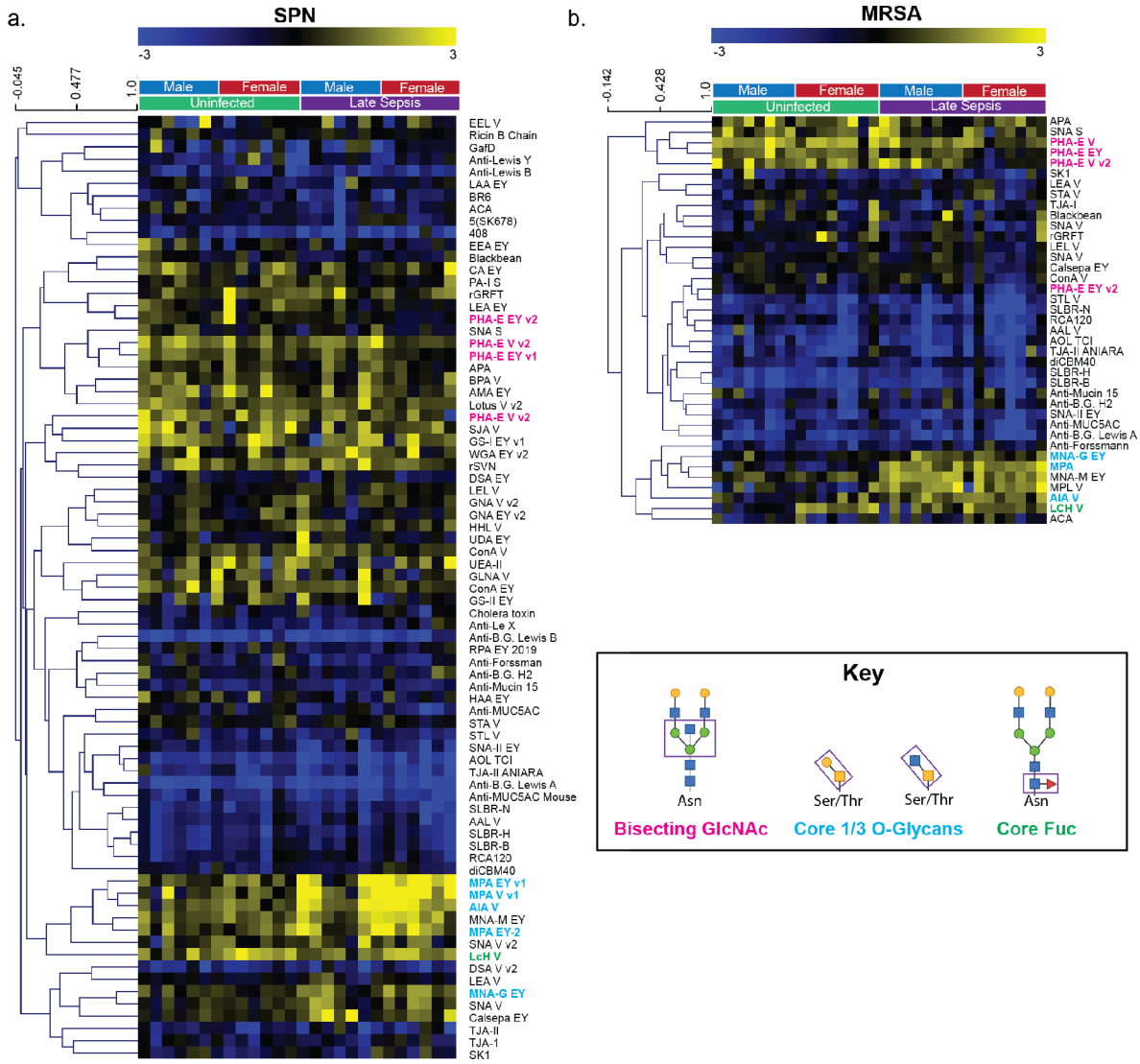

Figure 1. Heat map of lectin microarray data for Gram-positive bacteria. Median normalized $\log_2$ ratios (Sample (S)/Reference (R)) of mouse sera samples were ordered by uninfected or late sepsis for (a) SPN and (b) MRSA. Yellow, $\log_2(S) > \log_2(R)$; blue $\log_2(R) > \log_2(S)$. Lectins associated with bisecting GlcNAc (pink), Core 1/3 *O*-glycans (blue), and core fucose (green) are highlighted.

bacterial sepsis, we performed lectin microarray analysis on samples from ST and EC infected mice as previously described. Heatmaps are shown in Figures 2 and 3 and Supplementary Figures S6 and S7.

We observed conserved responses between Gram-negative and Gram-positive bacteria compared to the corresponding uninfected controls (Figures 2 and 3, Supplementary Figures S9 and S10). Again, one of the strongest changes observed in sepsis for both Gram-negative bacterial species was the increase in core 1/3 *O*-Glycans (MPA, AIA, MNA-G, ST: ~4-fold increase, $p = 0.01$, EC: ~1.5-fold increase, $p = 0.0001$). A decrease in bisecting GlcNAc epitopes was also observed (PHA-E, ST: ~1.5-fold decrease, $p = 0.03$, EC: ~1.5-fold decrease, $p = 0.0001$). In EC, but not ST, the response of core 1/3 *O*-Glycans and bisecting GlcNAc to infection could be clearly seen in early sepsis (Supplementary Figure S8). Of the

https://doi.org/10.1021/acsinfecdis.2c00082
ACS Infect. Dis. 2022, 8, 1075−1085

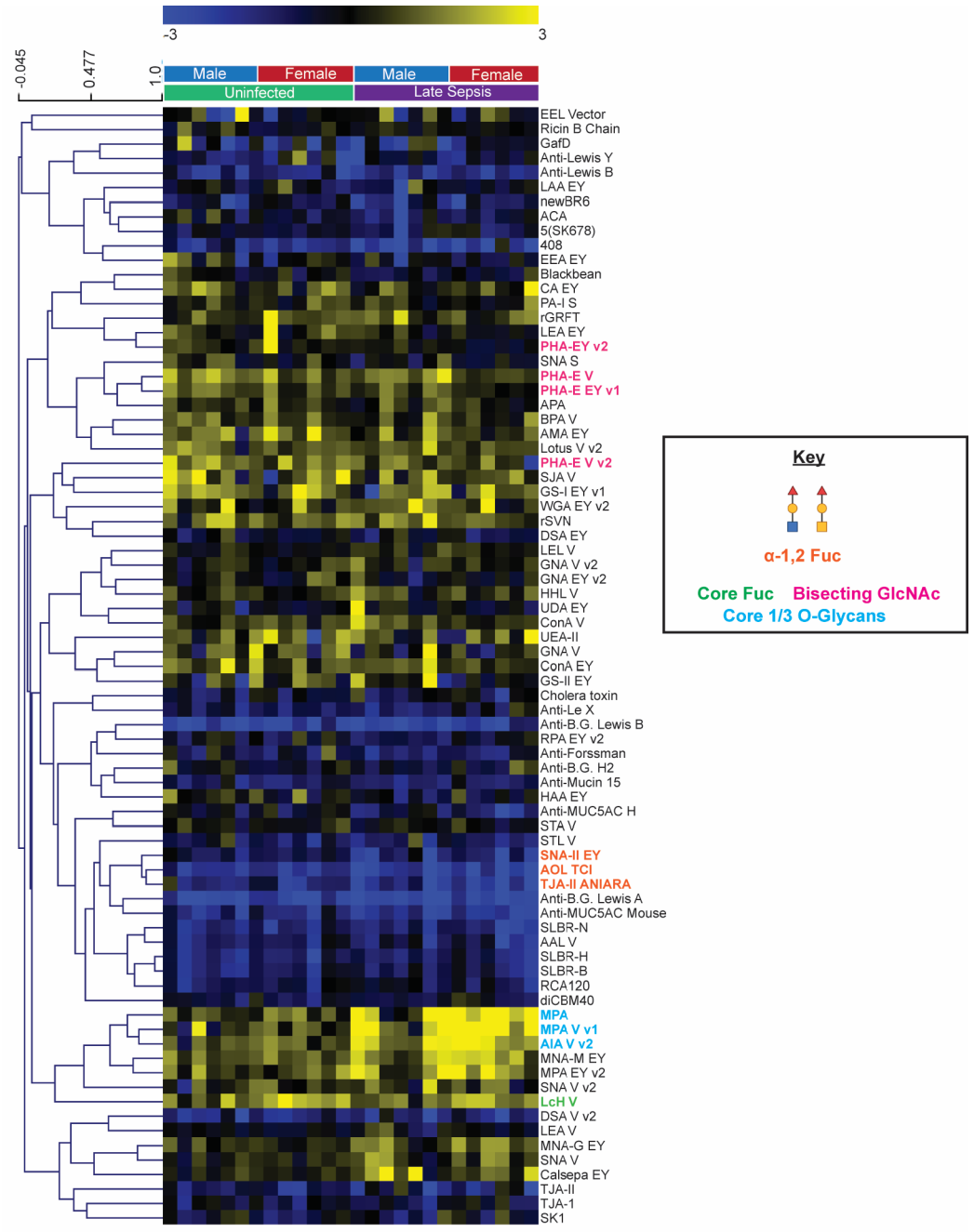

Figure 2. Heat map of lectin microarray data for sera from ST infected mice. Median normalized $\log_2$ ratios (Sample (S)/Reference (R)) of mouse sera samples were ordered by uninfected or late sepsis for (a) SPN and (b) MRSA. Yellow, $\log_2(S) > \log_2(R)$; blue $\log_2(R) > \log_2(S)$. Lectins associated with bisecting GlcNAc (pink), Core 1/3 *O*-glycans (blue), core fucose (green) and α-1,2 fucose (orange) are highlighted.

four bacteria studied, ST has the longest incubation period, due to its oral route of infection. Unlike the other bacteria where the early and late time points are 24 h apart, the two time points in ST are collected 3 days apart (Scheme 1). This may explain the delayed response observed.

Bacterial sepsis from ST and EC showed both overlapping and unique glycan signatures. Both Gram-negative bacteria induced a loss of α1,2-fucosylation (ST: ∼2-fold decrease, lectins: TJA-II, SNA-II, AOL, EC: ∼1.5-fold decrease, lectins: UEA-I, AAL, PTL-II). In the sera, α1,2-fucosylation is controlled by FUT2. This enzyme has a powerful role in the establishment and maintenance of the gut microbiota, which these two pathogens may affect. In recent work, α1,2-fucosylation has been found to increase colonization of *Salmonella* Typhimurium in a mouse model.[29] Conversely, the lack of FUT2, and thus sera α1,2-fucosylated glycans, is associated with an increase in severity for enteric EC infections.[30] The response to sepsis caused by EC was distinguishable from ST by additional changes in the serum glycome. EC-induced sepsis correlated with a loss of high- and oligomannose structures (GRFT, HHL, ConA, AMA, GNA), an increase in α2,6-sialic acids (SNA. TJA-I), a concomitant decrease in terminal β-galactose (RCA, ECA), and an increase in sulfated or α2,3-sialylated glycans (MAA, MAL-I). These differences were unique to sepsis caused by this bacterial pathogen.

https://doi.org/10.1021/acsinfecdis.2c00082
ACS Infect. Dis. 2022, 8, 1075−1085

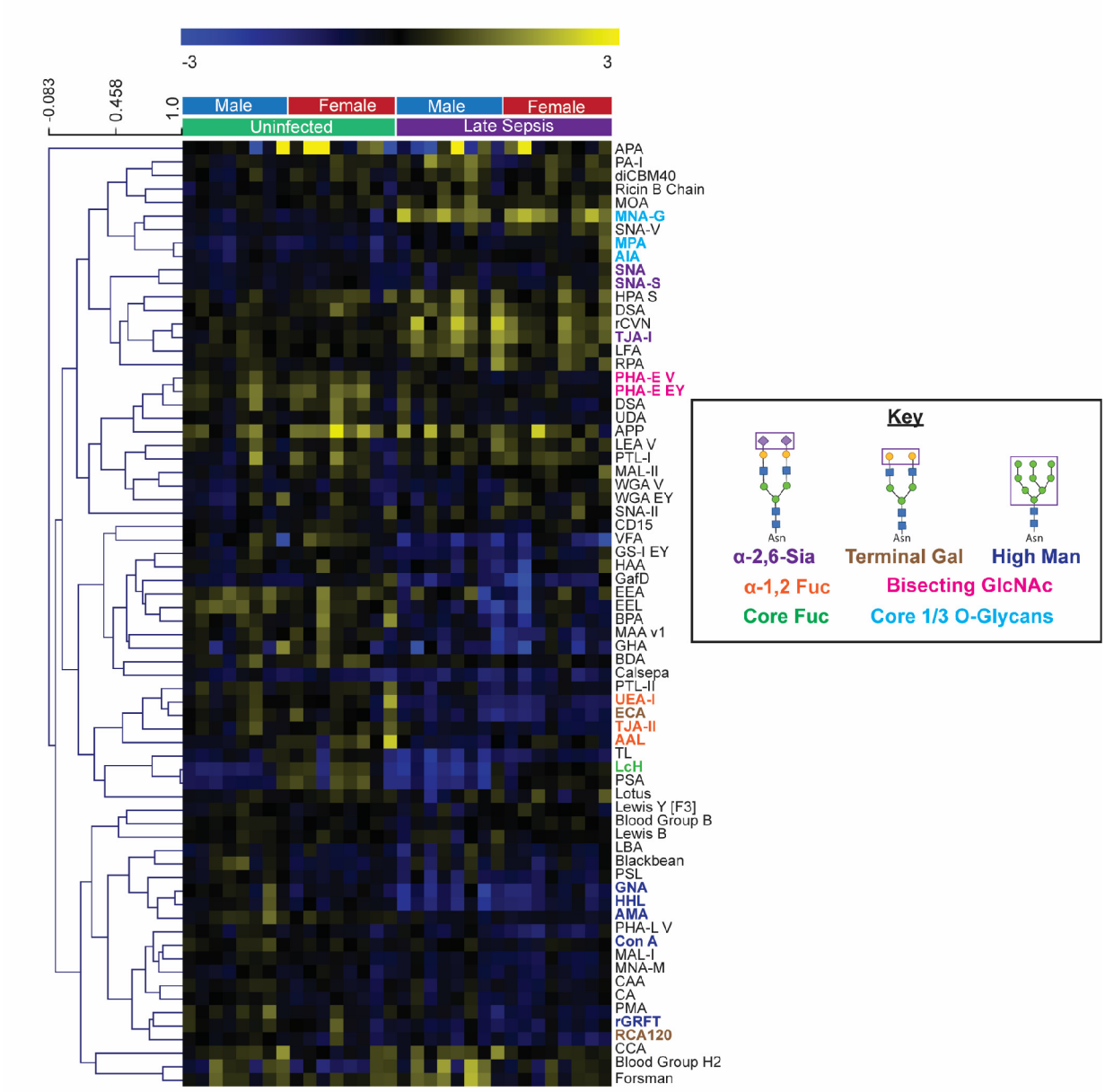

Figure 3. Heat map of lectin microarray data for sera from EC infected mice. Median normalized $\log_2$ ratios (Sample (S)/Reference (R)) of mouse sera samples were ordered by uninfected or late sepsis for (a) SPN and (b) MRSA. Yellow, $\log_2(S) > \log_2(R)$; blue $\log_2(R) > \log_2(S)$. Lectins associated with bisecting GlcNAc (pink), Core 1/3 *O*-glycans (blue), core fucose (green), α-1,2 fucose (orange) α-2,6 sialic acid (purple), terminal galactose (brown), and high mannose (blue) are highlighted.

Increase in Core 1/3 O-Glycans Is Conserved in Sepsis Across Bacterial Species. All four bacterial species studied cause a striking increase in core 1/3 *O*-glycan levels at late-stage sepsis, when signs of sepsis are visually overt (Figures 1−3 and 4a). Both AIA and MPA recognize these core 1/3 *O*-glycans with many terminal extensions, implying that expression of this epitope is likely due to an increase in levels of this *O*-glycan rather than trimming of existing unrecognized epitopes.[31] This effect on core 1/3 *O*-glycans is seen in both Gram-positive and Gram-negative infections. The increase of core 1/3 *O*-glycans can be observed in early sepsis in three out of the four organisms studied. The one exception is *Salmonella* Typhimurium, which may again be due to the longer incubation time for sepsis in this oral infection model.

To corroborate our lectin microarray analysis, we performed lectin blot analysis of mouse sera samples from our experimental models using the core 1/3 *O*-glycan binding lectin MPA. We did not observe a general increase in core 1/3 *O*-glycans across the molecular weight range in sepsis. Instead in all four experimental models, we observed what appears to be a single, high molecular weight band (>250 kDa, Figure 4b, Supplementary Figure S11). The staining of this band correlated with the observed MPA signal in our lectin microarrays. For example, in both our lectin blot and lectin microarray data, we detected a variable response in ST-induced sepsis. In cases where the lectin microarray found high levels of MPA, we observed high levels of the high MW glycoprotein in the MPA lectin blot and vice versa. This indicated that this

https://doi.org/10.1021/acsinfecdis.2c00082
ACS Infect. Dis. 2022, 8, 1075−1085

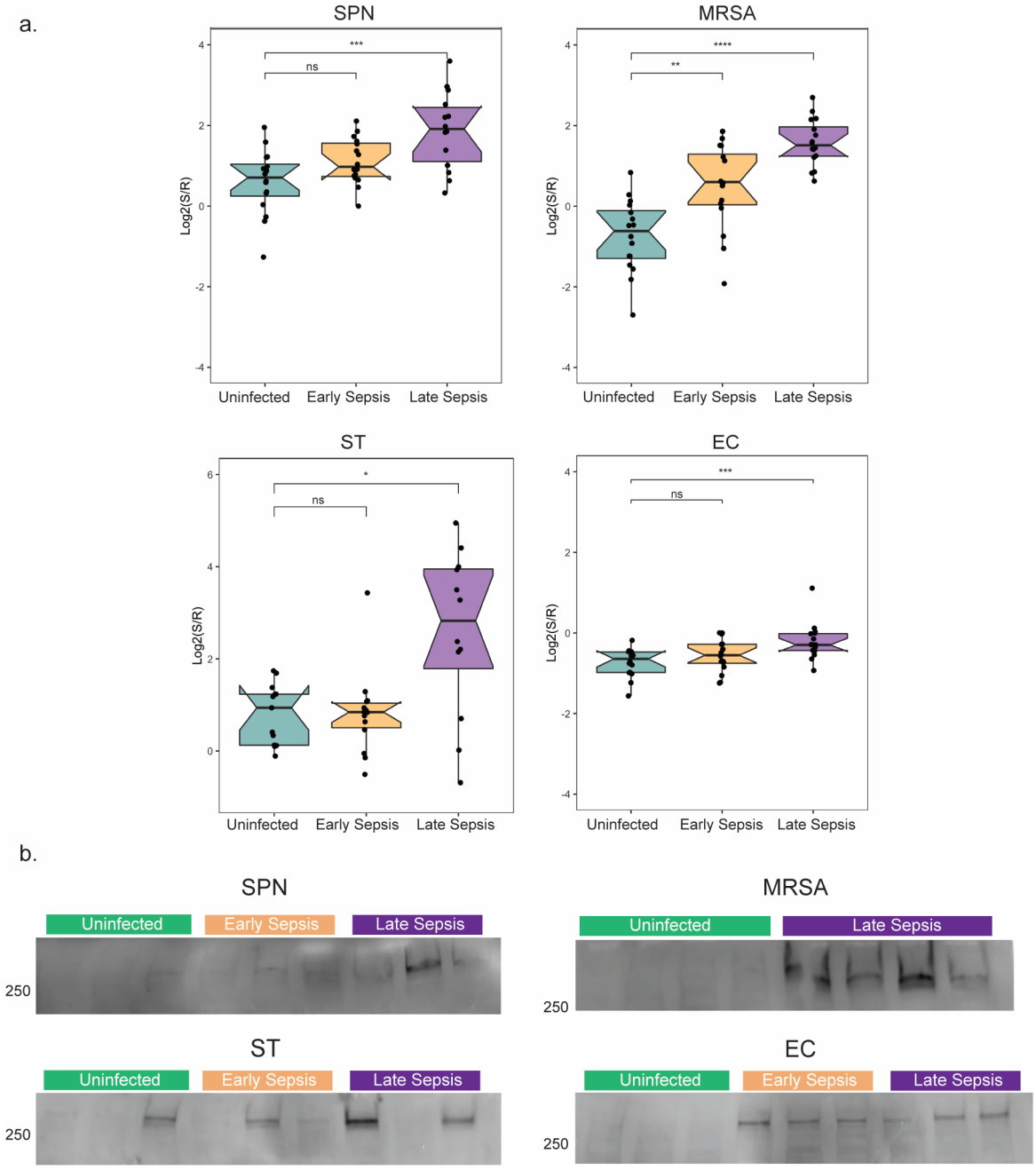

Figure 4. Core 1/3 *O*-glycan levels increase during sepsis. (a) Box plot analysis of lectin binding by MPA (core 1/3 *O*-glycans) are depicted. *P*-values derive from Student's *t* test (*$p \leq 0.05$, **$p \leq 0.01$, ***$p \leq 0.001$, ****$p \leq 0.0001$). (b) Lectin blots probed with biotinylated MPA and Streptavidin HRP show an increase in a single high molecular weight band in both early and late sepsis. Whole blots and corresponding Ponceau stained membranes are shown in Figure S11.

protein or proteins were responsible for the core 1/3 *O*-glycan signal.

Glycoproteomic Analysis Identifies O-Glycoproteins Elevated in Both Gram-Positive and Gram-Negative Induced Sepsis. We performed proteomic analysis of the high molecular weight MPA-enriched glycoproteins from our mouse sepsis models. Septic samples from all bacterial strains used in the study were pooled and enriched for core 1/3 O-glycosylated proteins using lectin chromatography with MPA. Proteins were then resolved on an SDS page gel and the high molecular weight band was excised for analysis by mass spectrometry (Figure 5a). Mass spectrometry identification found 24 proteins in total (Supplementary Tables S3 and S4). Of these, only 5 contained known glycosylation sites (Figure 5b). The top three proteins from our analysis, inter-α-trypsin inhibitor heavy chain 2 (ITIH2), fibronectin (FN1), and ITIH1 all have associations with bacterial sepsis and contain both *O*- and *N*-glycans.[32,33] ITIH1 and ITIH2 are both components of inter-α-trypsin inhibitor (IαI), which is known to bind extracellular matrix components including fibronectin and hyaluronan.[34] Loss of IαI in severe sepsis in human blood is correlated with higher mortality[34−38] and this protein is considered protective in mouse models. Similarly loss of fibronectin in human sera is also associated with higher mortality from sepsis.[39] In contrast to humans, in mouse models fibronectin is an acute phase protein, with higher levels

https://doi.org/10.1021/acsinfecdis.2c00082
ACS Infect. Dis. 2022, 8, 1075−1085

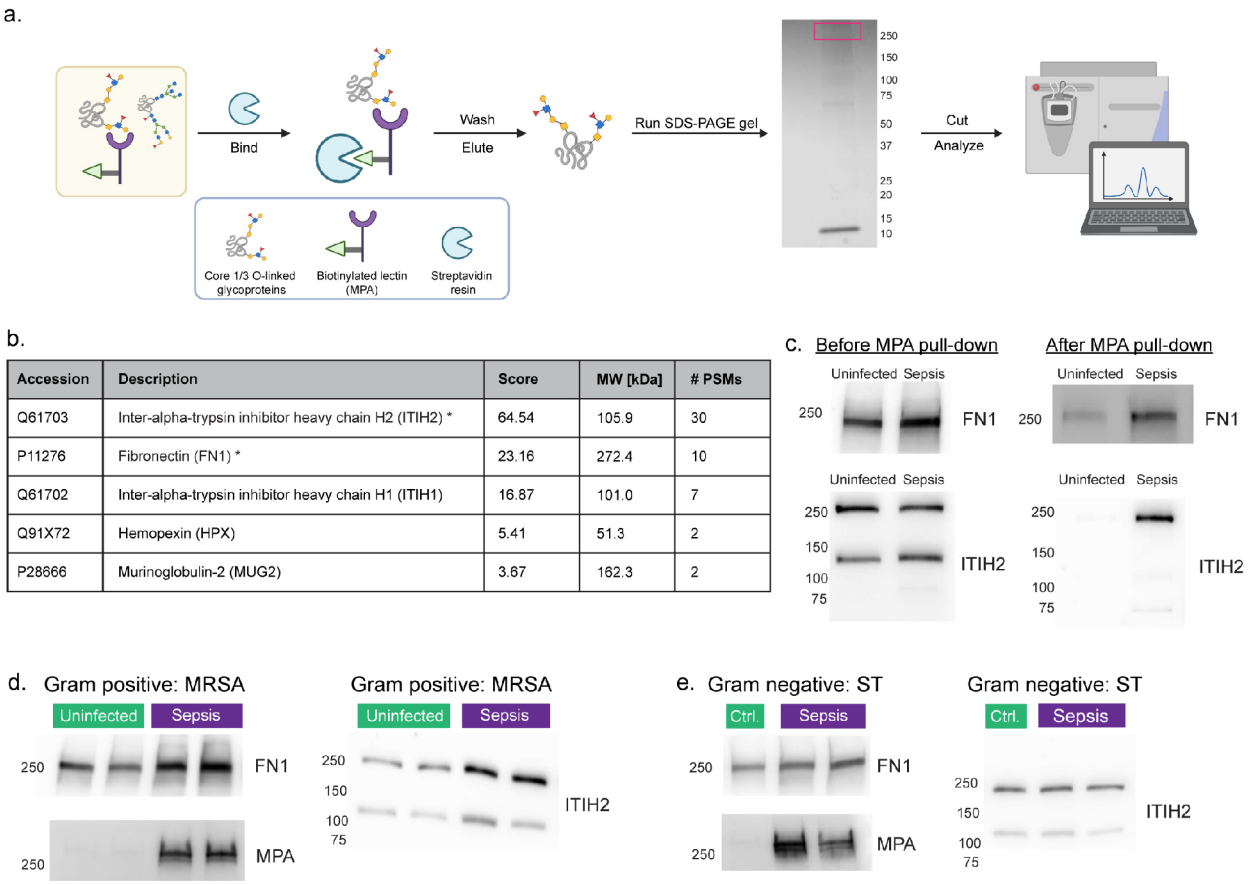

Accession	Description	Score	MW [kDa]	# PSMs
Q61703	Inter-alpha-trypsin inhibitor heavy chain H2 (ITIH2) *	64.54	105.9	30
P11276	Fibronectin (FN1) *	23.16	272.4	10
Q61702	Inter-alpha-trypsin inhibitor heavy chain H1 (ITIH1)	16.87	101.0	7
Q91X72	Hemopexin (HPX)	5.41	51.3	2
P28666	Murinoglobulin-2 (MUG2)	3.67	162.3	2

Figure 5. Glycoproteomic analysis identifies *O*-glycoproteins elevated in both Gram-positive and Gram-negative induced sepsis. (a) Schematic illustration of the experimental approach showing enrichment of core 1/3 O-glycosylated proteins by MPA lectin, and analysis by mass spectrometry. (b) List of glycoproteins identified in the core 1/3 O-linked glycans enriched septic samples. (c) MPA pulldown of pooled uninfected and septic samples followed by Western blot with anti-Fibronectin or anti-ITIH2 antibody. Entire blots and corresponding Ponceau stained membranes are shown in Figure S12. (d) Western Blot of Fibronectin and ITIH2, and Lectin Blot of MPA for sera from Gram-Positive: MRSA infected mice. (e) Western Blot of Fibronectin and ITIH2, and Lectin Blot of MPA for sera from Gram-Negative: ST infected mice. Entire blots and corresponding Ponceau stained membranes are shown in Figure S13.

correlated with inflammation.[40] The O-glycoforms of fibronectin alter epithelial-mesenchymal transition and may prevent protein degradation.[41,42] No information has been gathered about glycoform differences of these proteins and their potential influence on sepsis biology.

To validate our identification of these glycoproteins as core 1/3 O-glycosylated, we performed Western blot analysis on MPA pulldowns from pooled uninfected and sepsis samples. Both fibronectin and ITIH2 were preferentially pulled down in sepsis samples when compared to uninfected controls (Figure 5c, Supplementary Figure S12). For fibronectin, higher general levels of were seen in sepsis. However, stronger differences were seen in the pulldowns from the two pools, arguing some shift in glycoform. In contrast, our pooled septic and control samples showed even levels of ITIH2 protein, but dramatic differences in the levels pulled down by MPA. This provides clear evidence of a major glycoform shift to an MPA reactive core 1/3 *O*-glycan in ITIH2 during sepsis.

To better understand the interaction between changes in protein levels and glycosylation, we examined these glycoproteins in individual Gram-positive (MRSA) and Gram-negative (ST) samples. We observed a clear increase in overall fibronectin and ITIH2 signals in MRSA-induced sepsis that correlates with the increase in MPA observed (Figure 5d, Supplementary Figure S13a,c,e). However, the MPA staining changes more strongly than the protein levels, providing additional evidence for a change in glycoforms. In ST-induced sepsis, the increase in protein levels is clear for fibronectin, but not ITIH2 (Figure 5e, Supplementary Figure S13b,d,f).

Interestingly, although ITIH2 is known to have a molecular weight of 106 kDa, we observe two bands for this protein, one at ∼106 kDa and one at ∼250 kDa. One possibility is that we are observing a complex between fibronectin and ITIH2, however this is unlikely as the samples were boiled for 10 min under denaturing conditions. A second possibility is that we are observing ITIH2 in complex with α1-microglobulin as part of IαI. In that complex, ITIH1 and ITIH2 are both covalently linked through an ester bond to chondroitin sulfate chains on α1-microglobulin. Both ITIH2 and ITIH1 were observed in our mass spectrometry analysis. Our data suggest that in sepsis this complex is marked by a specific glycoform. Further research will be needed to explore these possibilities.

CONCLUSIONS

Bacterial sepsis is one of the top 10 causes of human death and disability, and its frequency is increasing with antibiotic resistance.[3,4] The Gram-positive (MRSA and SPN) and Gram-negative (EC and ST) bacterial pathogens used in our study are clinical isolates and common causes of human sepsis. At the molecular level, sepsis is incompletely defined, with a

https://doi.org/10.1021/acsinfecdis.2c00082
ACS Infect. Dis. 2022, 8, 1075−1085

descriptive rather than molecular diagnosis. Currently, there are few diagnostic biomarkers and with the exception of early application of antibiotics, targeted therapy has been ineffective.[1,2] There is a need to study further the molecular underpinnings of this syndrome. Glycosylation is known to play roles in immunity and inflammation, but the roles of glycans in sepsis are not well-defined. In this current study, we compared the sera glycomes of uninfected and septic mice across multiple bacterial strains (MRSA, SPN, EC, and ST) at two postinfection time points, tethered to increasing blood cfu levels.[9]

Using our lectin microarray platform, we observed major changes in the sera glycome that were conserved across all four experimental sepsis models, regardless of whether bacterial pathogens were Gram positive or negative. A common decrease in bisecting GlcNac and an increase in Core 1/3 *O*-glycans was associated with bacterial sepsis caused by multiple pathogens. These changes were visible at the earliest postinfection times studied. Lectin blot analysis using MPA identified what appears to be a conserved high molecular weight protein with elevated levels of core 1/3 *O*-glycans in sepsis caused by all bacteria studied.

Mass spectrometry analysis of the MPA binding fraction identified 3 major glycoproteins, fibronectin, ITIH2 and ITIH1. Both ITIH1 and ITIH2 are components of IαI, a hyaluronan binding protein associated with inflammatory processes. Fibronectin is an extracellular matrix protein that has differential associations with inflammatory processes in mouse and humans. All three of these proteins are associated with sepsis; however, we have little understanding of their glycoforms. Our data indicate that these proteins are glycosylated with core 1/3 *O*-glycans in sepsis and further suggest that there is a shift in glycosylation to a more O-glycosylated form for both fibronectin and ITIH2. Our data open up the possibility that this glycosylation shift impacts the biology of these proteins, an area for future investigations.

METHODS

Laboratory Animals. Animal studies were performed by the Marth laboratory at the University of California Santa Barbara. All studies were done with the approval of the Institutional Animal Care and Use Committees of the University of California Santa Barbara and the Sanford-Burnham-Prebys Medical Discovery Institute. Animal experiments were carried out with adult 8−12-week-old mice with equal numbers of male and female mice. Mice were provided sterile pellet food and water ad libitum. Littermates of four or five animals per cage were housed in a pathogen-free barrier facility at the University of California Santa Barbara.

Bacterial Strains and Culture Conditions. *Escherichia coli* (*EC*) strain ATCC 25922 (clinical isolate, FDA strain Seattle 1946), *Salmonella enterica* serovar Typhimurium (*ST*) reference strain ATCC 14028 (CDC 6516−60), *Streptococcus pneumoniae* (*SPN*) serotype 2 strain D39, and methicillin-resistant *Staphylococcus aureus* (*MRSA*) strain CA-MRSA USA300 were all used in these experiments.[18,43−46]

Bacterial Infections. All mice were infected and monitored as previously described[9] according to LD50 values that were predetermined for each bacterial species by identifying the dose at which 50% of infected animals died post infection by the specified delivery routes. *EC* and *SPN* bacterial strains were administered as an intraperitoneal (i.p.) infection with an *EC* dose at 10× LD50 and *SPN* dose at 10× LD50. Gastric intubation was used for the administration of *ST* at a dose of 20× LD50, or i.p. at a dose 20× LD50. Intravenous infection was utilized for *MRSA* infection at a dose of 20× LD50. Blood was collected and the bacterial cfu were measured at designated times postinfection. Mice that met minimal thresholds were utilized in this study and those outside of the target range were not analyzed further.

Lectin Microarray. Samples were labeled with Alexa Fluor 555-NHS. Serum protein concentrations were determined using the DC assay. 50 μg of protein were labeled for each individual sample following the manufacturers protocol. Reference samples were created for each bacterial experiment and labeled with Alexa Fluor 647-NHS. For SPN, MRSA, and ST, a bacteria-specific reference sample was prepared by mixing equal amounts of sera from all 48 animals used in each study, including uninfected controls. For EC, a master reference was created from the sera samples from the EC, ST and SPN experiments. Printing and hybridization were performed as previously described.[11,14,21,22] The printlists for our lectin microarrays are shown in Supplementary Table S1. For each lectin microarray experiment, only lectins that were active on >30% of all arrays were considered in the analysis. Log_2 values of the average signals for each lectin are median-normalized over the individual subarray in each channel. Hierarchical clustering using the Pearson Correlation Coefficient, heatmap generation and other data analysis was performed in R (version 3.6). Data annotation was done using the known specificities of the lectins.[31] We only annotated glycan changes that were consistent across genders, observed in lectins with similar binding motifs, where annotation was unambiguous, that had at least one probe that was statistically significant (as determined by Student *t* test), and where $a >$ 40% increase or decrease was observed.

Lectin Blots. Sera samples (3 per condition) with clear differences in MPA binding were chosen for lectin blot analysis. Serum protein concentrations were measured by DC assay (Biorad) and 20 μg of protein was resolved on an SDS page gel (gradient 4−20%, BioRad) and transferred to a nitrocellulose membrane. Protein loading was visualized using Ponceau staining.

For lectin blots shown in Figure 4: membranes were then blocked in 5% BSA in PBST (pH 7.4, 0.05% Tween-20) followed by washing with PBST (3×, 5 min). Biotinylated MPL (5 μg/mL, Vector Laboratories) was then added to the membrane in blocking buffer (1 h, RT) followed by washing with PBST (pH 7.4, 0.05% Tween-20, 3×, 5 min). Membranes were then incubated with Avidin-HRP (1:1000 in blocking buffer, ThermoFisher, 1 h, RT). For lectin blots shown in Figure 5: membranes were then blocked in 5% BSA in PBST (pH 7.4, 0.05% Tween-20) overnight at 4 °C followed by washing with PBST (3×, 5 min). Biotinylated MPL (1:1000 in blocking buffer, Vector Laboratories) was then added to the membrane in blocking buffer (1 h, RT) followed by washing with PBST (pH 7.4, 0.05% Tween-20, 3×, 5 min). Membranes were then incubated with Avidin-HRP (1:5000 in blocking buffer, ThermoFisher, 1 h, RT), and then followed by three washes with PBST. Blots were developed with SuperSignal West Femto (Thermo Scientific).

Western Blot of Lectin Immunoprecipitated Proteins. Equal volume of MPA immunoprecipitated proteins (10 μL) were resolved by SDS-PAGE gradient gel (Bio-Rad), transferred onto nitrocellulose membranes (ThermoFisher). Protein loading was visualized using Ponceau staining.

https://doi.org/10.1021/acsinfecdis.2c00082
ACS Infect. Dis. 2022, 8, 1075−1085

Membranes were then blocked in 5% milk in PBST (pH 7.4, 0.05% Tween-20) for 1 h at room temperature followed by washing with PBST (3×, 5 min). Antibodies were diluted in blocking buffer. Primary antibodies: rabbit polyclonal anti-Fibronectin (1:5000; Abcam, Ab2413), rabbit polyclonal anti-ITIH2 (1:5000; Abcam, Ab118257); 4 °C overnight. The blot was washed with PBST (3×, 5 min), then stained with secondary antibodies (antirabbit HRP; 1 h, RT; Cell signaling) in blocking buffer. Blots were developed using SuperSignal West Femto (ThermoFisher).

Western Blot of Gram-Positive and Gram-Negative Infected Sera Samples. Serum protein concentrations were determined by DC Assay (Biorad). Equivalent amounts (20 μg) of proteins were resolved by SDS-PAGE gradient gel (Bio-Rad), transferred onto nitrocellulose membranes (ThermoFisher). Protein loading was visualized using Ponceau staining. Membranes were then blocked in 5% milk in PBST (pH 7.4, 0.05% Tween-20) for 1 h at room temperature followed by washing with PBST (3×, 5 min). Antibodies were diluted in blocking buffer. Primary antibodies: rabbit polyclonal anti-Fibronectin (1:5000; Abcam, Ab2413), rabbit polyclonal anti-ITIH2 (1:5000; Abcam, Ab118257); 4 °C overnight. The blot was washed with PBST (3×, 5 min), then stained with secondary antibodies (antirabbit HRP; 1 h, RT; Cell signaling) in blocking buffer. Blots were developed using SuperSignal West Femto (ThermoFisher).

Glycoproteomic Pulldown and Analysis by Mass Spectrometry. A pool of uninfected samples was generated by taking equal amounts from individual serum samples. An orthogonal pool of septic samples was created by the same approach, and protein concentration was determined by DC Assay (Biorad). 1000 μg of pooled samples were mixed with 50 μL of biotinylated MPA lectin (stock concentration: 2 μg/μL, Vector Laboratories) and made up the volume to 200 μL with PBS containing 1% NP 40, and incubated at 4 °C overnight. Then 50 μL of settled Pierce Streptavidin Agarose Resins (ThermoFisher) was added, and incubated with mixing for 1 h at room temperature. The beads were washed with binding buffer (PBS containing 1% NP 40, 5 times) and subsequently extracted with SDS-PAGE sample buffer at 95 °C for 5−10 min.

Equal volumes of proteins (10 μL) were resolved by SDS-PAGE gradient gel (Bio-Rad), and visualized by Coomassie staining and Silver staining using standard protocols (ThermoFisher). The band at 250 kDa was excised and sent for analysis by mass spectrometry.

Samples were extracted from the gel, further reduced with DTT, alkylated with iodoacetamide, and trypsin digested. The resulting peptides were analyzed by nanoflow LC-MS using a data-dependent acquisition method on a Q Exactive mass spectrometer, described in more detail in the Supplemental Methods.

Proteomic Data Analysis. The raw data were searched against the Uniprot Human database (downloaded on May 12, 2016) using SEQUEST within Proteome Discoverer 1.4 (ThermoFisher). Data were filtered to exclude (1) known contaminants and (2) unglycosylated proteins. For more details, see Supplemental Methods.

■ ASSOCIATED CONTENT

Supporting Information

The Supporting Information is available free of charge at https://pubs.acs.org/doi/10.1021/acsinfecdis.2c00082.

Detailed sample preparation for mass spectrometry analysis (Supplementary Methods); data visualization of lectin microarray data for sera from 4 different clinical bacterial pathogens infected mice (Figure S1−S10); validation of lectin array by lectin blot and pull down assay (Figure S11−S13); lectin print list (Table S1); detailed lectin microarray information (Table S2); mass spectrometry analysis (Table S3) (PDF)

Glycoproteomic raw data (Table S4) (XLSX)

■ AUTHOR INFORMATION

Corresponding Author

Lara K. Mahal − *Biomedical Research Institute, Department of Chemistry, New York University, New York, New York 10003, United States; Department of Chemistry, University of Alberta, Edmonton, AB T6G 2G2, Canada;* orcid.org/0000-0003-4791-8524; Email: lkmahal@ualberta.ca

Authors

Daniel W. Heindel − *Biomedical Research Institute, Department of Chemistry, New York University, New York, New York 10003, United States*

Shuhui Chen − *Biomedical Research Institute, Department of Chemistry, New York University, New York, New York 10003, United States*

Peter V. Aziz − *SBP Medical Discovery Institute, La Jolla, California 92037, United States*

Jonathan Y. Chung − *Biomedical Research Institute, Department of Chemistry, New York University, New York, New York 10003, United States*

Jamey D. Marth − *SBP Medical Discovery Institute, La Jolla, California 92037, United States*

Complete contact information is available at: https://pubs.acs.org/10.1021/acsinfecdis.2c00082

Notes

The authors declare no competing financial interest.

■ ACKNOWLEDGMENTS

Research undertaken herein by J.D.M. and P.V.Z. was supported by NIH Grants HL131474 and DK048247. This research was also supported by funding from the Canada Excellence Research Chairs Program (L. Mahal). The mass spectrometric experiments are in part supported by the NYU Grossman School of Medicine, the Laura and Isaac Perlmutter Cancer Center Support Grant P30CA016087 from the National Cancer Institute, and a shared instrumentation grant from the NIH, 1S10OD010582-01A1, for the purchase of an Orbitrap Eclipse. Select figures are created with BioRender.

■ REFERENCES

(1) Marshall, J. C. Why have clinical trials in sepsis failed? *Trends Mol. Med.* **2014**, *20*, 195−203.

(2) Reyes, M.; Filbin, M. R.; Bhattacharyya, R. P.; Billman, K.; Eisenhaure, T.; Hung, D. T.; Levy, B. D.; Baron, R. M.; Blainey, P. C.; Goldberg, M. B.; Hacohen, N. An immune-cell signature of bacterial sepsis. *Nat. Med.* **2020**, *26*, 333−340.

(3) Chambers, H. F.; Deleo, F. R. Waves of resistance: Staphylococcus aureus in the antibiotic era. *Nat. Rev. Microbiol* **2009**, *7*, 629−641.

(4) Pradipta, I. S.; Sodik, D. C.; Lestari, K.; Parwati, I.; Halimah, E.; Diantini, A.; Abdulah, R. Antibiotic resistance in sepsis patients:

evaluation and recommendation of antibiotic use. *N Am. J. Med. Sci.* **2013**, *5*, 344−352.
(5) van der Poll, T.; Opal, S. M. Host-pathogen interactions in sepsis. *Lancet Infect Dis* **2008**, *8*, 32−43.
(6) Marth, J. D.; Grewal, P. K. Mammalian glycosylation in immunity. *Nat. Rev. Immunol* **2008**, *8*, 874−887.
(7) Chacko, B. K.; Scott, D. W.; Chandler, R. T.; Patel, R. P. Endothelial surface N-glycans mediate monocyte adhesion and are targets for anti-inflammatory effects of peroxisome proliferator-activated receptor gamma ligands. *J. Biol. Chem.* **2011**, *286*, 38738−38747.
(8) Scott, D. W.; Vallejo, M. O.; Patel, R. P. Heterogenic endothelial responses to inflammation: role for differential N-glycosylation and vascular bed of origin. *J. Am. Heart Assoc.* **2013**, *2*, e000263.
(9) Yang, W. H.; Heithoff, D. M.; Aziz, P. V.; Haslund-Gourley, B.; Westman, J. S.; Narisawa, S.; Pinkerton, A. B.; Millan, J. L.; Nizet, V.; Mahan, M. J.; Marth, J. D. Accelerated Aging and Clearance of Host Anti-inflammatory Enzymes by Discrete Pathogens Fuels Sepsis. *Cell Host Microbe* **2018**, *24*, 500−513.
(10) Takao, K.; Miyakawa, T. Genomic responses in mouse models greatly mimic human inflammatory diseases. *Proc. Natl. Acad. Sci. U. S. A.* **2015**, *112*, 1167−1172.
(11) Pilobello, K. T.; Slawek, D. E.; Mahal, L. K. A ratiometric lectin microarray approach to analysis of the dynamic mammalian glycome. *Proc. Natl. Acad. Sci. U. S. A.* **2007**, *104*, 11534−11539.
(12) Batista, B. S.; Eng, W. S.; Pilobello, K. T.; Hendricks-Munoz, K. D.; Mahal, L. K. Identification of a conserved glycan signature for microvesicles. *J. Proteome Res.* **2011**, *10*, 4624−4633.
(13) Krishnamoorthy, L.; Bess, J. W., Jr; Preston, A. B.; Nagashima, K.; Mahal, L. K. HIV-1 and microvesicles from T cells share a common glycome, arguing for a common origin. *Nat. Chem. Biol.* **2009**, *5*, 244−250.
(14) Koppolu, S.; Wang, L.; Mathur, A.; Nigam, J. A.; Dezzutti, C. S.; Isaacs, C.; Meyn, L.; Bunge, K. E.; Moncla, B. J.; Hillier, S. L.; Rohan, L. C.; Mahal, L. K. Vaginal Product Formulation Alters the Innate Antiviral Activity and Glycome of Cervicovaginal Fluids with Implications for Viral Susceptibility. *ACS Infect Dis* **2018**, *4*, 1613−1622.
(15) Agrawal, P.; Fontanals-Cirera, B.; Sokolova, E.; Jacob, S.; Vaiana, C. A.; Argibay, D.; Davalos, V.; McDermott, M.; Nayak, S.; Darvishian, F.; Castillo, M.; Ueberheide, B.; Osman, I.; Fenyo, D.; Mahal, L. K.; Hernando, E. A Systems Biology Approach Identifies FUT8 as a Driver of Melanoma Metastasis. *Cancer Cell* **2017**, *31*, 804−819.
(16) Bird-Lieberman, E. L.; Neves, A. A.; Lao-Sirieix, P.; O'Donovan, M.; Novelli, M.; Lovat, L. B.; Eng, W. S.; Mahal, L. K.; Brindle, K. M.; Fitzgerald, R. C. Molecular imaging using fluorescent lectins permits rapid endoscopic identification of dysplasia in Barrett's esophagus. *Nat. Med.* **2012**, *18*, 315−321.
(17) Grewal, P. K.; Aziz, P. V.; Uchiyama, S.; Rubio, G. R.; Lardone, R. D.; Le, D.; Varki, N. M.; Nizet, V.; Marth, J. D. Inducing host protection in pneumococcal sepsis by preactivation of the Ashwell-Morell receptor. *Proc. Natl. Acad. Sci. U. S. A.* **2013**, *110*, 20218−20223.
(18) Grewal, P. K.; Uchiyama, S.; Ditto, D.; Varki, N.; Le, D. T.; Nizet, V.; Marth, J. D. The Ashwell receptor mitigates the lethal coagulopathy of sepsis. *Nat. Med.* **2008**, *14*, 648−655.
(19) Weiser, J. N.; Ferreira, D. M.; Paton, J. C. Streptococcus pneumoniae: transmission, colonization and invasion. *Nat. Rev. Microbiol* **2018**, *16*, 355−367.
(20) Bogaert, D.; De Groot, R.; Hermans, P. W. Streptococcus pneumoniae colonisation: the key to pneumococcal disease. *Lancet Infect Dis* **2004**, *4*, 144−154.
(21) Pilobello, K. T.; Agrawal, P.; Rouse, R.; Mahal, L. K. Advances in lectin microarray technology: optimized protocols for piezoelectric print conditions. *Curr. Protoc Chem. Biol.* **2013**, *5*, 1−23.
(22) Pilobello, K. T.; Krishnamoorthy, L.; Slawek, D.; Mahal, L. K. Development of a lectin microarray for the rapid analysis of protein glycopatterns. *Chembiochem* **2005**, *6*, 985−989.
(23) Irvine, E. B.; Alter, G. Understanding the role of antibody glycosylation through the lens of severe viral and bacterial diseases. *Glycobiology* **2020**, *30*, 241−253.
(24) Zou, G.; Ochiai, H.; Huang, W.; Yang, Q.; Li, C.; Wang, L. X. Chemoenzymatic synthesis and Fcgamma receptor binding of homogeneous glycoforms of antibody Fc domain. Presence of a bisecting sugar moiety enhances the affinity of Fc to FcgammaIIIa receptor. *J. Am. Chem. Soc.* **2011**, *133*, 18975−18991.
(25) Bermejo-Martin, J. F.; Giamarellos-Bourboulis, E. J. Endogenous immunoglobulins and sepsis: New perspectives for guiding replacement therapies. *Int. J. Antimicrob. Agents* **2015**, *46*, S25−S28.
(26) Abe, R.; Oda, S.; Sadahiro, T.; Nakamura, M.; Hirayama, Y.; Tateishi, Y.; Shinozaki, K.; Hirasawa, H. Gram-negative bacteremia induces greater magnitude of inflammatory response than Gram-positive bacteremia. *Crit Care* **2010**, *14*, R27.
(27) Hartman, M. E.; Linde-Zwirble, W. T.; Angus, D. C.; Watson, R. S. Trends in the epidemiology of pediatric severe sepsis*. *Pediatr Crit Care Med.* **2013**, *14*, 686−693.
(28) Vincent, J. L.; Martinez, E. O.; Silva, E. Evolving concepts in sepsis definitions. *Crit Care Clin* **2009**, *25*, 665−675.
(29) Suwandi, A.; Galeev, A.; Riedel, R.; Sharma, S.; Seeger, K.; Sterzenbach, T.; Garcia Pastor, L.; Boyle, E. C.; Gal-Mor, O.; Hensel, M.; Casadesus, J.; Baines, J. F.; Grassl, G. A. Std fimbriae-fucose interaction increases Salmonella-induced intestinal inflammation and prolongs colonization. *PLoS Pathog* **2019**, *15*, No. e1007915.
(30) Mottram, L.; Wiklund, G.; Larson, G.; Qadri, F.; Svennerholm, A. M. FUT2 non-secretor status is associated with altered susceptibility to symptomatic enterotoxigenic Escherichia coli infection in Bangladeshis. *Sci. Rep.* **2017**, *7*, 10649.
(31) Bojar, D.; Meche, L.; Meng, G.; Eng, W.; Smith, D. F.; Cummings, R. D.; Mahal, L. K. A Useful Guide to Lectin Binding: Machine-Learning Directed Annotation of 57 Unique Lectin Specificities. *ACS Chem. Biol.* **2022**, DOI: 10.1021/acschembio.1c00689.
(32) Liu, D.; Wang, S.; Zhang, J.; Xiao, W.; Miao, C. H.; Konkle, B. A.; Wan, X. F.; Li, L. Site-Specific N- and O-Glycosylation Analysis of Human Plasma Fibronectin. *Front Chem.* **2021**, *9*, 691217.
(33) Flahaut, C.; Capon, C.; Balduyck, M.; Ricart, G.; Sautiere, P.; Mizon, J. Glycosylation pattern of human inter-alpha-inhibitor heavy chains. *Biochem. J.* **1998**, *333*, 749−756.
(34) Lord, M. S.; Melrose, J.; Day, A. J.; Whitelock, J. M. The Inter-alpha-Trypsin Inhibitor Family: Versatile Molecules in Biology and Pathology. *J. Histochem Cytochem* **2020**, *68*, 907−927.
(35) Lim, Y. P.; Bendelja, K.; Opal, S. M.; Siryaporn, E.; Hixson, D. C.; Palardy, J. E. Correlation between mortality and the levels of inter-alpha inhibitors in the plasma of patients with severe sepsis. *J. Infect Dis* **2003**, *188*, 919−926.
(36) Opal, S. M.; Lim, Y. P.; Siryaporn, E.; Moldawer, L. L.; Pribble, J. P.; Palardy, J. E.; Souza, S. Longitudinal studies of inter-alpha inhibitor proteins in severely septic patients: a potential clinical marker and mediator of severe sepsis. *Crit Care Med.* **2007**, *35*, 387−392.
(37) Mizon, C.; Piva, F.; Queyrel, V.; Balduyck, M.; Hachulla, E.; Mizon, J. Urinary bikunin determination provides insight into proteinase/proteinase inhibitor imbalance in patients with inflammatory diseases. *Clin. Chem. Lab. Med.* **2002**, *40*, 579−586.
(38) Wu, R.; Cui, X.; Lim, Y. P.; Bendelja, K.; Zhou, M.; Simms, H. H.; Wang, P. Delayed administration of human inter-alpha inhibitor proteins reduces mortality in sepsis. *Crit. Care Med.* **2004**, *32*, 1747−1752.
(39) Lemanska-Perek, A.; Krzyzanowska-Golab, D.; Skalec, T.; Adamik, B. Plasma and Cellular Forms of Fibronectin as Prognostic Markers in Sepsis. *Mediators Inflamm.* **2020**, *2020*, 8364247.
(40) Lemanska-Perek, A.; Adamik, B. Fibronectin and its soluble EDA-FN isoform as biomarkers for inflammation and sepsis. *Adv. Clin Exp Med.* **2019**, *28*, 1561−1567.
(41) Freire-de-Lima, L.; Gelfenbeyn, K.; Ding, Y.; Mandel, U.; Clausen, H.; Handa, K.; Hakomori, S. I. Involvement of O-glycosylation defining oncofetal fibronectin in epithelial-mesenchymal

transition process. *Proc. Natl. Acad. Sci. U. S. A.* **2011**, *108*, 17690−17695.
(42) Park, J. H.; Katagiri, T.; Chung, S.; Kijima, K.; Nakamura, Y. Polypeptide N-acetylgalactosaminyltransferase 6 disrupts mammary acinar morphogenesis through O-glycosylation of fibronectin. *Neoplasia* **2011**, *13*, 320−326.
(43) Beumer, C.; Wulferink, M.; Raaben, W.; Fiechter, D.; Brands, R.; Seinen, W. Calf intestinal alkaline phosphatase, a novel therapeutic drug for lipopolysaccharide (LPS)-mediated diseases, attenuates LPS toxicity in mice and piglets. *J. Pharmacol Exp Ther* **2003**, *307*, 737−744.
(44) Chow, O. A.; von Kockritz-Blickwede, M.; Bright, A. T.; Hensler, M. E.; Zinkernagel, A. S.; Cogen, A. L.; Gallo, R. L.; Monestier, M.; Wang, Y.; Glass, C. K.; Nizet, V. Statins enhance formation of phagocyte extracellular traps. *Cell Host Microbe* **2010**, *8*, 445−454.
(45) Heithoff, D. M.; Shimp, W. R.; House, J. K.; Xie, Y.; Weimer, B. C.; Sinsheimer, R. L.; Mahan, M. J. Intraspecies variation in the emergence of hyperinfectious bacterial strains in nature. *PLoS Pathog* **2012**, *8*, e1002647.
(46) van Sorge, N. M.; Beasley, F. C.; Gusarov, I.; Gonzalez, D. J.; von Kockritz-Blickwede, M.; Anik, S.; Borkowski, A. W.; Dorrestein, P. C.; Nudler, E.; Nizet, V. Methicillin-resistant Staphylococcus aureus bacterial nitric-oxide synthase affects antibiotic sensitivity and skin abscess development. *J. Biol. Chem.* **2013**, *288*, 6417−6426.

https://doi.org/10.1021/acsinfecdis.2c00082
ACS Infect. Dis. 2022, 8, 1075−1085